ACTA MECHANICA SINICA (English Series), Vol.16, No.4, November 2000 ISSN 0567-7718
The Chinese Society of Theoretical and Applied Mechanics
Chinese Journal of Mechanics Press, Beijing, China
Allerton Press, INC., New York, U.S.A.

MOLECULAR DYNAMICS SIMULATION OF THE ROLE OF DISLOCATIONS IN MICROCRACK HEALING*

Li Shen (李 深) Gao Kewei (高克玮) Qiao Lijie (乔利杰) Chu Wuyang (褚武扬)
(Dept. of Mater. Phys., Univ. of Sci. Tech., Beijing, Beijing 100083, *China)*

Zhou Fuxin (周富信)
(LNM Inst. of Mech., CAS, Beijing 100080, *China)*

ABSTRACT: The molecular dynamics method is used to simulate microcrack healing during heating or/and under compressive stress. A centre microcrack in Cu crystal would be sealed under compressive stress or by heating. The role of compressive stress and heating in crack healing was additive. During microcrack healing, dislocation generation and motion occurred. When there were pre-existing dislocations around the microcrack, the critical temperature or compressive stress necessary for microcrack healing would decrease, and, the higher the number of dislocations, the lower the critical temperature or compressive stress. The critical temperature necessary for microcrack healing depended upon the orientation of the crack plane. For example, the critical temperature for the crack along the (001) plane was the lowest, i.e. 770K.

KEY WORDS: microcrack healing, molecular dynamics simulation, dislocation

1 INTRODUCTION

Microcracks in ceramic[1~3], plexiglass[4], and ice[5] could be healed through atom diffusion during heating. Microcrack in metal materials can also be healed. For example, for hot-rolled inconel 600 alloy, microcracks originated early at the grain boundary were closed during heating over 870°C with large compressive stress by moving grain boundaries in the process of recrystallization[6]. For Cu30Fe duplex alloy, microcracks formed early during rolling at room temperature could be closed after rolling exceeded 30%[7]. For 20 MnMo steel, microcracks disappeared during hot deformation[8]. *In situ* TEM observations showed that for metal materials, whether ductile or brittle, dislocation emission and motion occurred before and during crack initiation or/and propagation[9~11]. Therefore, the resistance for crack propagation is $2\gamma + \gamma_p$, where γ is the surface energy and γ_p the plastic work. What remains to be elucidated is whether the dislocation emission and motion are involved in microcrack closure or healing; or whether the plastic work is also involved in the resistance required for microcrack healing.

Received 17 February 2000, revised 6 June 2000
* The project supported by the Special Fund for the Major State Basic Research Projects (No. G19990650) and by the National Natural Science Foundation of China (No. 19891180, 59871010)

Dislocation emission and crack propagation can be simulated by the molecular dynamics method[12~14]. In the present paper, the molecular dynamics method is used to simulate microcrack healing during pressing or heating and to reveal the role of plastic deformation in microcrack healing.

2 COMPUTATION PROCEDURE

Copper was chosen as the simulated material. The interatomic potential used here is the N-body potential proposed by Finnis and Sinclair[15] according to the embedded atom method (EAM) and constructed by Ackland et al.[16]. The inner atoms follow law of Newton, i.e.

$$F_i = -\frac{\partial E_{\mathrm{tot}}}{\partial r_i} = m_i \frac{\mathrm{d}v_i}{\mathrm{d}t} \tag{1}$$

Where E_{tot} is the total energy of a system of atoms in the EAM and m_i is the mass of the i-th atom. The leapfrog algorithm[7] is applied to calculate the positions r_i and velocities of atoms, i.e.

$$\begin{aligned} v_i(t+\Delta t/2) &= (1-\eta)v_i(t-\Delta t/2) + (F_i/m_i)\Delta t \\ r_i(t+\Delta t) &= r_i(t) + v_i(t+\Delta t/2)\Delta t \\ v_i(t+\Delta t) &= [v_i(t+\Delta t/2) + v_i(t-\Delta t/2)]/2 \end{aligned} \tag{2}$$

where $\eta = 0.1$ for relaxation processes and $\eta = 0$ for loading processes. The above scheme provides an update formulation from the current time. The initial velocity is the Maxwell-Boltzmann distribution corresponding to a given temperature. The system temperature is maintained at a constant value during simulations.

The parallelepiped with a center slit is used as the simulated cell in the present calculations. The x, y and z axes are along the extension line of the center crack, along the normal of the crack plane, and along the $[11\bar{2}]$ direction, respectively. The inclination angle between the (111) slip plane and the crack plane changes from 0° to 90° and, in general, is set to be 70°. The length of the crystal along $[\bar{1}10]$ is 45 periods, the width along [111] is 25 periods, and the thickness along $[11\bar{2}]$ is one period. The number of atoms used here is about 6000. The length of the center crack is $2a = 3.6\,\mathrm{nm}$, and the width is 0.6 nm, which is larger than the potential cutoff distance, which is 0.44 nm.

The displacement boundary condition is to be used. The atoms move according to the plane strain linear elastic displacement field for a cracked solid[18], which is of the form

$$\begin{aligned} u &= \frac{1+\nu}{E}[(1-2\nu)\mathrm{Re}\bar{Z} - y\mathrm{Im}Z] \\ v &= \frac{1+\nu}{E}[2(1-\nu)\mathrm{Im}\bar{Z} - y\mathrm{Re}Z] \\ w &= 0 \end{aligned} \tag{3}$$

where $Z = \sigma z/\sqrt{(z+a)(z-a)}$, $Z \equiv \mathrm{d}\bar{Z}/\mathrm{d}z$, $z = x + \mathrm{i}y$, σ is the applied stress, a is the half-length of the center crack, E is the Young's modulus and ν is the Poisson's ratio. Along z-direction, a six layer periodic representation is applied.

For the displacement boundary, the edge-cracked crystal is likely to emit dislocations during mode I loading[12~14] but cannot be closed, and for the center-cracked crystal, the situation is quite the opposite. In order to generate dislocations in the center-cracked crystal, the edge-cracked crystal is used to emit dislocations under mode I loading, and then the atomic configuration in the area containing the dislocations, which contains 24×24 rows atoms, is copied to the center-cracked crystal. During coping, the relative displacements between boundary atoms of the area containing the dislocations and their nearest atoms in the case of edge-cracked crystal are the same as those in the case of center-cracked crystal.

3 SIMULATED RESULTS

3.1 Crack Healing by Heating

The inclination angle between the crack plane and the (111) slip plane is 70°. After the center slit is formed, the configuration is relaxed at 0 K until reaching equilibrium, as shown in Fig.1(a). The temperature is chosen to be 600 K, 650 K, 700 K, 750 K and 800 K respectively, and maintained to constant during relaxation. The time step is 7.5×10^{-4}ps. Simulations show that when temperature is maintained at 600 K, 650 K and 700 K, the center crack can not close after relaxing for a long time, as shown in Fig.1(b). If the temperature is maintained at 750 K, the crack begins to heal after relaxing for 3 ps along with generating dislocations, as shown in Fig.2(a). After 7.5 ps, the crack is approximately healed but a void V and some dislocations as B, C, and D are left, as shown in Fig.2(b). The void does not disappear after relaxing for a long time at 750 K. At 800 K, the crack is completely closed after relaxing for 9 ps, and some dislocations such as A, B, C, D, E, F and G are left, but

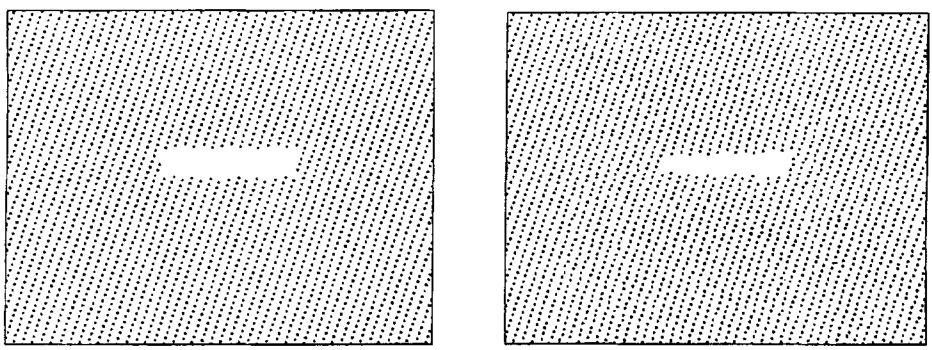

(a) (b)

Fig.1 The atomic configuration obtained by relaxing at 0 K (a) and at 700 K (b)

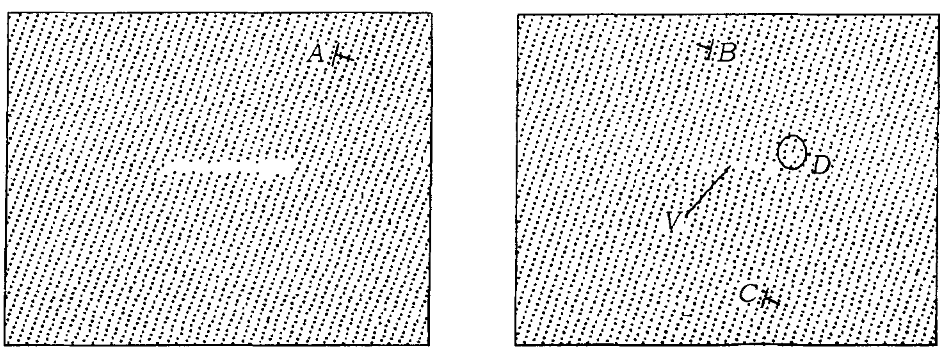

(a) (b)

Fig.2 Crack healing by heating after relaxing for 3 ps at 750K(a), for 7.5ps at 750K(b), and for 9ps at 800K(c). A to G are dislocations and V void

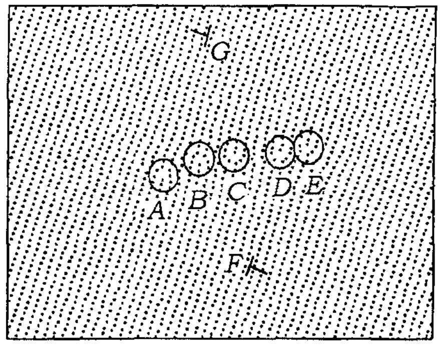

(c)

Fig.2 Crack healing by heating after relaxing for 3 ps at 750 K(a), for 7.5ps at 750 K(b), and for 9ps at 800 K(c). A to G are dislocations and V void (continued)

no void, as shown in Fig.2(c).

3.2 Crack Healing by Compressive Stress

A compressive stress σ perpendicular to the crack plane is applied with a loading rate of 0.13 GPa/ps. When the compressive stress increases to $\sigma = -7.26\,\mathrm{GPa}$, the crack heals to some extent but a void and some dislocations are left, as shown in Fig.3(a). When compressive stress is increased to $\sigma = -13.2\,\mathrm{GPa}$, the crack closes completely, and some dislocations but no void remain in the crystal, as shown in Fig.3(b).

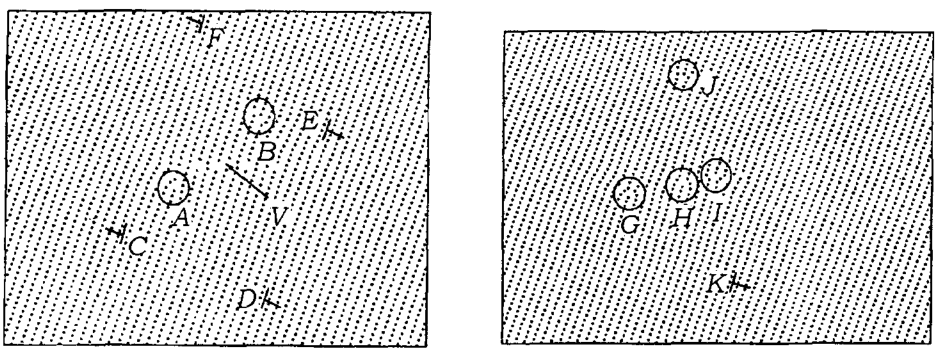

(a) (b)

Fig.3 Crack healing under compressive stress of 7.26 GPa at 0 K (a) and 13.2 GPa at 0 K (b). A to K are dislocations, V void

3.3 Crack Healing During Heating under Compressive Stress

Simulations show that the critical compressive stress and critical temperature necessary for crack healing are $\sigma_c = -13.2\,\mathrm{GPa}$ and $T_c = 800\,\mathrm{K}$, respectively. If compressive stress $\sigma = -3.96\,\mathrm{GPa}$ is applied and temperature is maintained at 600 K, the crack is completely closed after relaxing for 11.25 ps and some dislocations are left, as shown in Fig.4. Therefore, the applied compressive stress of 3.96 GPa can decrease the critical temperature necessary for crack healing from 800 K to 600 K. Figure 4 also indicates that increasing the temperature from 0 K to 600 K can reduce the critical compressive stress necessary for crack healing from 13.2 GPa to 3.96 GPa.

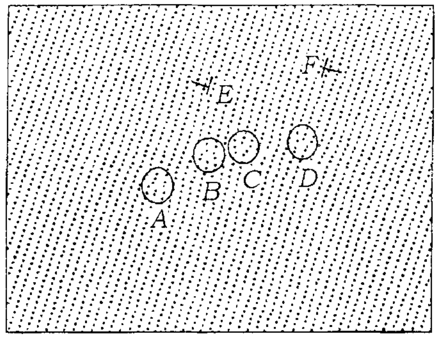

Fig.4 Crack healing at 600 K under $\sigma = -3.96\,\mathrm{GPa}$. A to D are Frank dislocations, E and F Shockley dislocations

3.4 Effect of Orientation of the Crack Plane on Crack Healing

If the crack plane is along the (111) slip plane ($\theta = 0$), the critical temperature necessary for crack healing is 850 K instead of 800 K, as shown in Fig.5(a). Crack healing at 850 K is also accompanied with the generation and movement of dislocations.

If the crack plane is along (001) plane ($\theta = 54.7°$), the critical temperature for crack healing is 770 K, as shown in Fig.5(b). When the crack plane is along the $[\bar{1}\,10]$ plane, ($\theta = 90°$), the critical temperature for crack healing is 790 K, as shown in Fig.5(c).

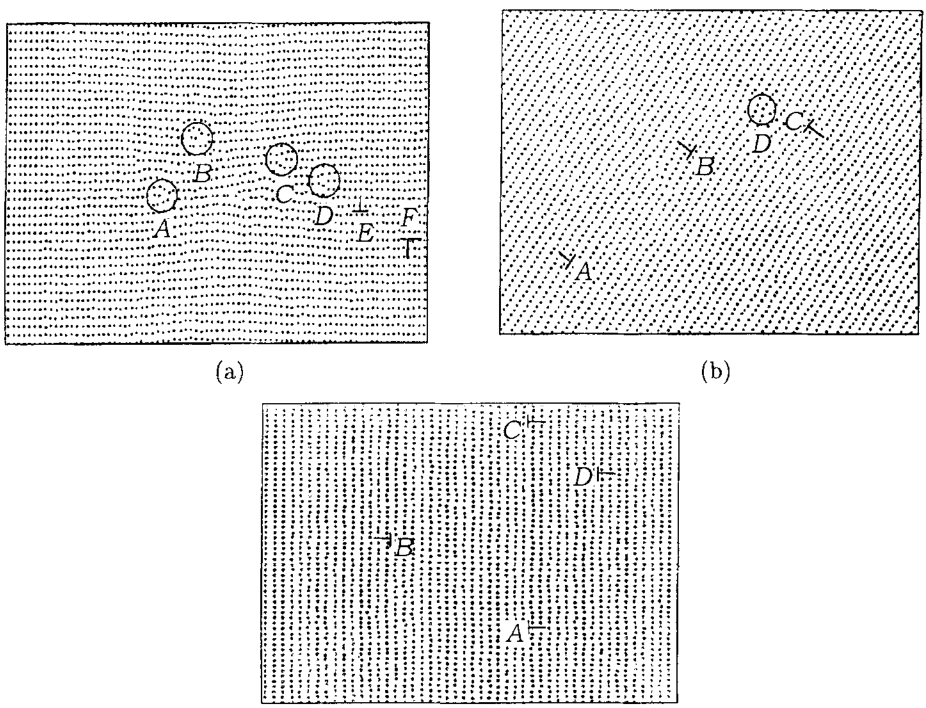

(a) (b)

(c)

Fig.5 Healing of the crack along the (111) plane at 850K(a), the (001) plane at 770 K and the $(\bar{1}10)$ plane at 790 K(c)

3.5 Effect of Dislocation on Crack Healing

For the edge-cracked crystal, a tensile stress perpendicular to the crack plane is applied with a loading rate of 0.01 MPa$\sqrt{\text{m}}$/ps. When K_I = 0.5 MPa$\sqrt{\text{m}}$ corresponding to 10 000 time steps, the first Shockley dislocation is emitted from the crack tip, and when K_I = 0.6 MPa$\sqrt{\text{m}}$, two Shockley dislocations are emitted from the tip of the edge crack, as shown in Fig.6(a). The atomic configuration of the edge-cracked crystal in area A, which contains the two dislocations, is copied to the center-cracked crystal, and an equilibrium atom configuration can be obtained after relaxing at 0 K for a long time, as shown in Fig.6(b).

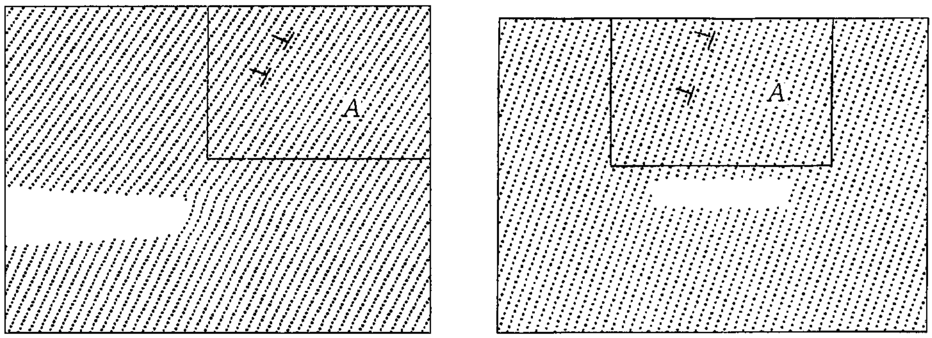

(a) edge crack (b) center crack

Fig.6 The atomic configuration containing two dislocations

For the center-cracked crystal containing no dislocation, the critical temperature for crack healing is 800 K, as shown in Fig.2(c). However, when the center-cracked crystal containing two Shockley dislocations is maintained at 650 K, the crack begins to heal after 2 500 time steps. At the same time, the pre-existing dislocations have disappeared and some new dislocations have appeared. After relaxing at 650 K for 10 000 time steps, the crack is completely closed and some new dislocations form, as shown in Fig.7(a). This shows that two pre-existing dislocations can reduce the critical temperature necessary for crack healing from 800 K to 650 K. For the center-cracked crystal without dislocations, the critical compressive stress necessary for crack healing at 0 K is $\sigma = -13.2$ GPa, as shown in Fig.3(b). If there are two pre-existing dislocations, the crack will be completely closed under a compressive stress $\sigma = -9.9$ GPa at 0 K, as shown in Fig.7(b). This indicates that two pre-existing dislocations can decrease the critical compressive stress for crack healing from 13.2 GPa to 9.9 GPa. In other words, pre-existing dislocations can promote crack healing. If the atomic configuration in the area A shown in Fig.6(a) is copied twice to the center-cracked crystal, there are four pre-existing dislocations. At 500 K, the crack has been completely closed after relaxing for 6500 time steps and some dislocations are generated, as shown in Fig.7(c). Therefore, pre-existing dislocation can decrease the critical temperature for crack healing, and the higher the number of the pre-existing dislocations, the lower the critical temperature for crack healing.

4 DISCUSSION

Similar to crack propagation, crack healing must overcome the surface energy 2γ. On the other hand, our simulations show that crack healing is accompanied with dislocation generation and movement, which involves the plastic deformation work γ_p. Hence, the resistance of crack healing is $2\gamma + \gamma_p$.

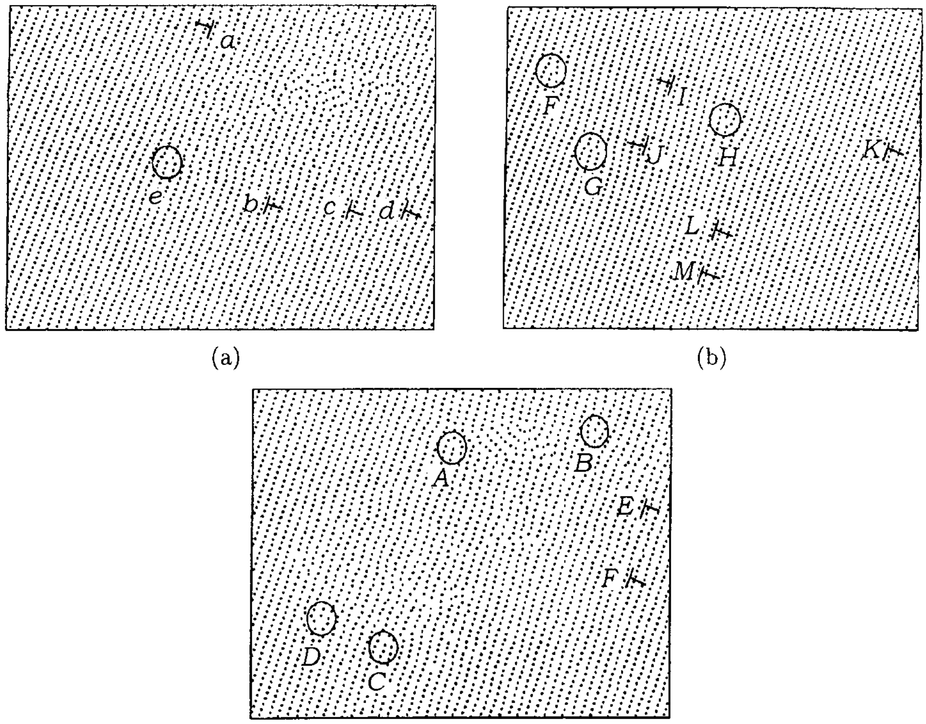

Fig.7 Crack healing for the crystal containing two dislocations at 650 K(a), at 0 K but under a compressive stress of 9.9 GPa(b), and containing four dislocations at 500 K(c)

Applied compressive stress σ can cause crack healing, as shown in Fig.3. Therefore, the elastic energy $\sigma^2\pi a(1-\nu^2)/E$ is a driving force for crack healing. On the other hand, only heating can cause crack healing up, hence $\partial U_T/\partial A$, where U_T is the thermal energy related to crack close and A is the area of the crack, is also the driving force for crack healing. Figure 4 indicates that compressive stress can decrease the critical temperature for crack healing, and increasing the temperature can reduce the critical compressive stress for crack healing. This shows that the two driving forces are additive. Therefore, the condition for crack healing is as follows

$$\frac{\sigma^2\pi a(1-\nu^2)}{E} + \frac{\partial U_T}{\partial A} \geq 2\gamma + \gamma_p \tag{3}$$

Since the surface energy γ is anisotropic, the critical temperature necessary for crack healing is related with the orientation of the crack plane. For Cu, the crack along the (001) plane is the easiest to heal, and the critical temperature for crack healing is the lowest (see Fig.5). Figure 7 shows that pre-existing dislocations could reduce the critical temperature or the critical compressive stress for crack healing. Equation (3) clearly shows that pre-existing dislocations can reduce the resistance of crack healing, that is, reduce the plastic work γ_p.

5 CONCLUSIONS

(1) Compressive stress or heating can cause a center crack healing, and their role are additive;

(2) Crack healing is accompanied with the generation and movement of dislocations;

(3) The critical temperature of crack healing is related with the orientation of the crack plane;

(4) Pre-existing dislocations can reduce the critical temperature necessary for crack healing.

REFERENCES

1 Wang Z, Li Y Z, Harmer M P, Chou Y T. Thermal healing of laser-induced internal cracks in lithiumfluoride crystals. *J Amer Ceram Soc*, 1992, 74: 1596

2 Gupta T K. Crack healing in thermally shocked MgO. *J Amer Ceram Soc*, 1975, 58: 143

3 Thompson A M, Chan H M, Harmer M P. Crack healing and stress relaxation in Al_2O_3-SiC nanocomposites. *J Amer Ceram Soc*, 1995, 78: 567

4 Holden M K C, Frechette V D. Crack healing in plexigrass. *J Ceram Soc Amer*, 1989, 72: 2189

5 Colbeck S C. Theory of microfracture healing in ice. *Acta Metall*, 1986, 34(1): 89

6 Shapiro E, Dieter G E. High temperature high strain rate fracture of inconel 600. *Metall Tran*, 1970, 1: 1711

7 Foct J, Akdut N, Gottstein G. Why are duplex microstructures easter to form than expected. *Scr Meta Mater*, 1992, 27: 1033

8 Han J T, Zhao G, Cao Q X. A regularity of crack healing for 20MnMo steel. *Science in China*, 1997, 27E: 23

9 Chen Q Z, Chu W Y, Hsiao C M. In situ TEM observations of nucleation and bluntness of nanocracks in thin crystal of 310 stainless stel. *Acta Metall*, 1995, 43: 4371

10 Chen Q Z, Gao K W, Zhang Y, Chu W Y. Nucleation blunting and propagation of a nanocrack in DFZ of thin crystals. *Fat Fract Eng Mater Stru*, 1998, 21: 1415

11 Gao K W, Chu W Y, Wang Y B. In situ TEM observation of dislocation-enhanced dislocation emission, motion and the nucleation of SCC for Ti-24Al-11Nb alloy in methanol. *Scripta Mater*, 1997, 36: 259

12 Hoagland R G, Daw M S, Foiles S M, Baskes M I. An atomic model of crack tip deformation in Al using an embedded atom potential. *J Mater Sci*, 1990, 5: 313

13 Zhang Y W, Wang T C, Tang Q H. Brittle and ductile fracture at the atomistic crack tip in copper crystals. *Scripta Mater*, 1995, 33: 267

14 Kitagawa H, Nakatani A, Shibutani Y. Molecular dynamics study of crack processes associated with dislocation nucleated at the tip. *Mater Sci Eng A*, 1994, 176: 263

15 Finnis M W, Sinclair J E. A simple N-body potential for transition metals. *Phil Mag*, 1984, A50: 45

16 Ackland G J, Tichy G, Vitek V, Finnis M W. Simpl N-body potentials for the noble metals and nickel. *Phil Mag*, 1987, A56: 735

17 Heermann D W. Computer Simulation Methods in Theoretic Physics. 2nd Edition. Berlin: Springer-Verlag, 1990

18 Knott J F. Fundamentals of Fracture Mechanics. London: Butterworth and Co. Ltd, 1973. 54